FEBS Letters 589 (2015) 910–918

FEBS Letters

journal homepage: www.FEBSLetters.org

Improved O_2-tolerance in variants of a H_2-evolving [NiFe]-hydrogenase from *Klebsiella oxytoca* HP1☆

Gang-Feng Huang [a], Xiao-Bing Wu [a,*], Li-Ping Bai [a], Ke Liu [a], Li-Jing Jiang [b], Min-Nan Long [c], Qing-Xi Chen [a,*]

[a] State Key Laboratory of Cellular Stress Biology and Key Laboratory of the Ministry of Education for Coastal and Wetland Ecosystems, School of Life Sciences, Xiamen University, Xiamen 361102, China
[b] Key Laboratory of Marine Biogenetic Resources, Third Institute of Oceanography, State Oceanic Administration, Xiamen 361005, China
[c] School of Energy Research, Xiamen University, Xiamen 361102, China

ARTICLE INFO

Article history:
Received 30 January 2015
Revised 14 February 2015
Accepted 23 February 2015
Available online 3 March 2015

Edited by Miguel De la Rosa

Keywords:
H_2-evolving hydrogenase
O_2-tolerance
Mutation
Gas channel
Biocatalysts
Klebsiella oxytoca HP1

ABSTRACT

In this study, we investigated the mechanism of O_2 tolerance of *Klebsiella oxytoca* HP1 H_2-evolving hydrogenase 3 (KHyd3) by mutational analysis and three-dimensional structure modeling. Results revealed that certain surface amino acid residues of KHyd3 large subunit, in particular those at the outer entrance of the gas channel, have a visible effect on its oxygen tolerance. Additionally, solution pH, immobilization and O_2 partial pressure also affect KHyd3 O_2-tolerance to some extent. We propose that the extent of KHyd3 O_2-tolerance is determined by a balance between the rate of O_2 access to the active center through gas channels and the deoxidation rate of the oxidized active center. Based on our findings, two higher O_2-tolerant KHyd3 mutations G300E and G300M were developed.

1. Introduction

Hydrogenases can catalyze the reversible reaction between H_2 and H^+ ($H_2 \leftrightarrow 2H^+ + 2e^-$) [1]. Currently, research on hydrogenases is a hotspot because they can be used as biocatalysts in H_2-based biotechnology [2–8], especially in biofuel cells [9–11]. Improving O_2-tolerance of hydrogenases is a major challenge because O_2-sensitivity largely hinders their real applications. Although O_2-sensitve hydrogenases could conduct good short-term performance in enzyme fuel cell, in order to have good long-term performance still need to address the root cause of O_2-sensitivity [12].

A lot of work has been devoted to understanding molecular basis of hydrogenases' O_2-sensitivity with the aim of developing high O_2-tolerant hydrogenases [13,14]. There were two hypotheses for the mechanism of hydrogenases' O_2-sensitivity. One was that hydrogenases' O_2-tolerance was mainly due to the effect of gas channels, which restricted O_2 access to active center via gas channels. Some studies demonstrated that certain hydrogenases were slowly inactivated by O_2 because the diffusion rate of O_2 to the active center via gas channels was lower [5,13–20]. Some AARs which located at inner exit of gas channels next to the active-center were found. They impacted hydrogenases' O_2-tolerance by restricting O_2 access to active center via gas channels (diminished channel diameters) [15–20]. The other one was that hydrogenases' O_2-tolerance mainly originated from the reductive removal of oxygenic species from oxygen-bound Ni–Fe active-center guided by a unique architecture of the electron relay. A series of studies

Abbreviations: AARs, amino acid residues; GC, gas chromatograph; HA, hydrogenase activity; HY, hydrogen yield; HycE, large subunit of KHyd3; HycG, small subunit of KHyd3; Hyd3, hydrogenase 3; KHyd3, *Klebsiella oxytoca* HP1 hydrogen-evolving hydrogenase 3; MBH, membrane banding hydrogenase; MhycE, mutated *hyc*E gene; ND, not detectable; OE-PCR, overlap extension polymerase chain reaction; RYY, ratio of aerobic HY to anaerobic HY; RAA, ratio of initial HA to residual HA; RH, regulatory [NiFe]-hydrogenase; SA, sodium alginate; SH, sensor hydrogenases; TiO_2, titanium dioxide; WT (K), wild-type *K. oxytoca* HP1; WT (E),

☆ Author contributions: Conceived and designed the experiments: Gang-Feng Huang, Xiao-Bing Wu, Qing-Xi Chen. Performed the experiments: Gang-Feng Huang, Li-Ping Bai, Ke Liu. Analyzed the data: Gang-Feng Huang, Li-Ping Bai, Xiao-Bing Wu. Contributed reagents/materials/analysis tools: Li-Jing Jiang, Min-Nan Long. Wrote the paper: Gang-Feng Huang, Xiao-Bing Wu.

* Corresponding authors. Fax: +86 592 2185487.
E-mail addresses: wuxiaobing@xmu.edu.cn (X.-B. Wu), chenqx@xmu.edu.cn (Q.-X. Chen).

http://dx.doi.org/10.1016/j.febslet.2015.02.027

revealed a Fe–S electron transfer relay; in particular, a special proximal [4Fe–3S] cluster (covalently binded by six cysteines (Cys) rather than four conservative Cys) close to the active site was closely related to O_2-tolerance [13,21–27]. Extra cysteines would be conducive to stabilizing the whole electron relay (Fe–S clusters) and delivering extra electrons towards the active-center via modification of Fe–S clusters [23,27]. Therefore, they will be beneficial to removing oxygenic species from the active center by reduction reaction (transformed O to H_2O with enough electrons) when O_2 attacked the active center.

We previously reported an O_2-tolerant H_2-evolving [NiFe]-hydrogenase from *Klebsiella oxytoca* HP1 [28,29]. *Escherichia coli* and *K. oxytoca* HP1 both belong to the *Enterobacteriaceae* family. Although *E. coli* possesses four different hydrogenase gene clusters (*hya*, *hyb*, *hyc* and *hyf*) [30,31], there was only one hydrogenase gene cluster in *K. oxytoca* HP1, which is highly similar to the *hyc* of *E. coli*. The *hyc* operon in *E. coli* contains eight genes (*hyc*A, *hyc*B, *hyc*C, *hyc*D, *hyc*E, *hyc*F, *hyc*G, *hyc*H and *hyc*I) [31]. All of these *hyc* genes were also present in *K. oxytoca* HP1 (Supplementary Table S1 and Fig. S1). The *hyc*E gene of *E. coli* encoded the large subunit of hydrogenase 3 (Hyd3) (an O_2-sensitive [NiFe]-hydrogenase) in which a Ni–Fe active center was buried, and *hyc*G gene encoded the small subunit which contained Fe–S clusters with electron-transferring function [30,31]. Although amino acid sequences of HycE and HycG subunits from *K. oxytoca* HP1 are highly similar with that of *E. coli* (Supplementary Table S1), Hyd3s of them showed significantly different O_2-tolerance. Hyd3 of *E. coli* was promptly inactivated when being exposed to air atmosphere, however, Hyd3 of *K. oxytoca* HP1 still showed high O_2-tolerance in the same atmosphere [29]. *K. oxytoca* HP1 also exhibited substantial H_2-evolving activity in 10% O_2 or air atmosphere [29,32] (Supplementary Table S2).

We had preliminary verified that KHyd3's HycE and HycG subunits were crucial for aerobic hydrogen production in our published work [32]. Additionally, we had improved O_2-tolerance of KHyd3 by Gly-Cys exchanges nearby Fe–S clusters in KHyd3's small subunit (HycG) [33]. However, O_2-tolerant molecular basis of KHyd3 is still unclear. Thus, this time we further investigated the role of KHyd3's large subunit (HycE) to uncover its O_2-tolerant mechanism. In this paper, we used Hyd3 of *E. coli* as a comparison (an O_2-sensitive [NiFe]-hydrogenase), finding key AARs relating to the O_2-tolerance of KHyd3 through site-directed mutagenesis analysis and homology modeling analysis. Our purpose was to further study its O_2-tolerant mechanism and to provide a theoretical basis to further develop highly O_2-tolerant KHyd3 variants as biocatalysts.

2. Materials and methods

2.1. Strains and growth conditions

K. oxytoca HP1 and *E. coli* have been conserved in our laboratory. Mutated strains grew anaerobically in Luria–Bertani (LB) medium with tetracycline (20 μg/mL) at 37 °C. The hydrogen production medium consisted of $MgSO_4{\cdot}7H_2O$ (0.37 g/L), KH_2PO_4 (3.63 g/L), $Na_2HPO_4{\cdot}12H_2O$ (14.33 g/L) and glucose (10 g/L) [32].

2.2. Site-directed mutagenesis

Mutated *hyc*E gene (*Mhyc*E) was generated by overlap extension polymerase chain reaction (OE-PCR) [34]. The homologous recombination plasmid contained two homologous recombination arm genes (arm 1: *Mhyc*E; arm 2: *hyc*FG) and a selection-marker gene (*tet*). The recombinant *Mhyc*E-*tet*-*hyc*FG fragment was generated by double digestion reaction from the recombinant plasmid

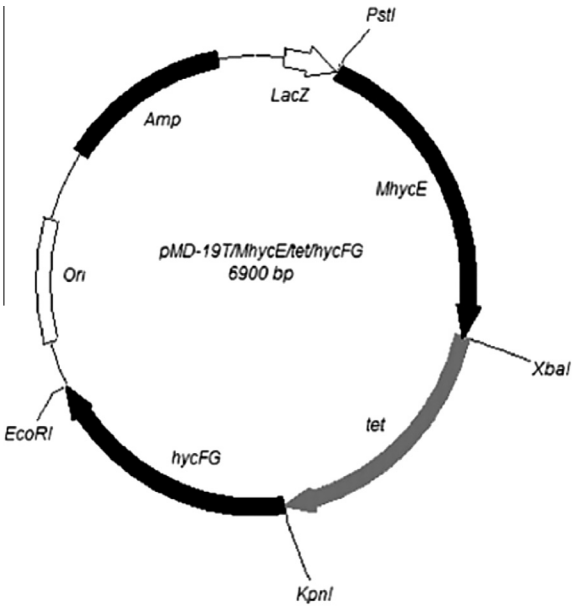

Fig. 1. Construction of recombination plasmid.

(Fig. 1). Then it was transferred into *K. oxytoca* HP1 and *E. coli* to generate corresponding mutations based on double homologous recombination technology. Variants were screened by tetracycline-resistant media, PCR techniques and sequencing. Details of site-directed mutagenesis were described in Supplementary methods.

2.3. Hydrogenase activity and oxygen tolerance analysis

Methods of hydrogenase purification and enzyme activity assay referred to our previous work [28,29]. The main steps of hydrogenase purification described as below [18,19]: (1) harvesting cells and resuspending them in pH 7.5 50 mM Tris–HCl buffer (containing 2 mM DTT and 1 mM PMSF); (2) disrupting cells by sonication (300 W, 20 kHz, min; JY92-II, Scientz) at 0 °C for 40–50 min; (3) collecting the supernatant by ultracentrifugation (400,000×*g*, 4 °C, 1 h); (4) purifying samples by DEAE-Sepharose FF (Amersham-Pharmacia, Sweden) column (2.6 × 20 cm) (equilibrating it with pH 7.5 50 mM Tris-buffer (containing 2 mM DTT and 1 mM PMSF); conducting a linear salt gradient washing (0–0.2 M NaCl); collecting the fractions with enzyme activity); (5) purifying the enzyme samples to butyl 4 sepharose FF (Amersham-Pharmacia) column (2.6 × 5 cm) (equilibrating it with pH 7.5 50 mM Tris–HCl buffer (containing 1 M $(NH_4)_2SO_4$; eluting it by 50 mL Tris–HCl (-containing 0.5 M $(NH_4)_2SO_4$, Tris–HCl supplemented with 0.2 M $(NH_4)_2SO_4$), Tris–HCl with 0.1 M $(NH_4)_2SO_4$ (3 mL/min) and then a 150 mL volume of a linear salt gradient (0.1–0 M $(NH_4)_2SO_4$); collecting the fractions with enzyme activity and then recovered and dialyzed them via 2 L pH 7.5 50 mM Tris–HCl buffer (4 °C, 4 h)); (6) purifying the dialyzed extract by SOURCE 30 Q (Amersham-Pharmacia) column (2.6 × 5 cm) (eluting it with 100 mL pH 7.5 50 mM Tris–HCl buffer for three times (containing 0.05 M NaCl, 0.1 M NaCl and 1 M NaCl, respectively); collecting hydrogenase samples and ultrafiltered them); (7) purifying hydrogenase samples by Sephacryl 200 column (1 × 120 cm), (eluting it with pH 7.5 50 mM Tris–HCl buffer (containing 0.1 M NaCl) (0.3 mL/min); collecting fractions with enzyme activity and then were pooled, concentrated and stored at 4 °C. The main procedure of enzyme activity assay described as below [28,29,32]: (1) Tris–HCl (pH 7.5, 50 mM), purified enzyme sample, methyl viologen (1.5 mM) and

sodium dithionite (25 mM) were added to the 5 mL plain tube; (2) the tube pumped with argon to maintain an anaerobic environment; (3) the tube was kept in a water bath (37 °C) for 30 min; (4) the accumulated H_2 was detected by gas chromatography (GC; GC9790, Fuli Instrument Company, China).

Ratio of aerobic hydrogen yield to anaerobic hydrogen yield [33] (RYY, RYY (%) = (aerobic hydrogen yield in a given time/anaerobic hydrogen yield in a given time) × 100%) and ratio of initial hydrogenase activity to residual hydrogenase activity [33] (RAA, RAA (%) = (the specific enzyme activity of the purified hydrogenase at a given time after exposure to air/the initial specific enzyme activity of the purified hydrogenase before exposure to air) × 100%) were used, respectively, to assess oxygen tolerance in vivo and in vitro.

2.4. Hydrogenase immobilization

100 mg titanium dioxide (TiO_2) was sonicated in 10 mL pH 7.5 50 mM Tris–HCl buffer. Then 10 mL hydrogenase sample was added into the stirred dispersion. The mixture was left stirring for 1 h at 4 °C [33]. After centrifuging, TiO_2-hydrogenase particles were resuspended into 10 mL pH 7.5 50 mM Tris–HCl buffer to conduct O_2-tolerant test [33].

Hydrogenase was embedded in sodium alginate (SA) by the following method. SA aqueous solution (3.5% w/v) was mixed with equal volume hydrogenase solution in a 37 °C water bath. The mixture was drawn into a syringe (5 mL) and then injected into $CaCl_2$ aqueous solution (2% w/v) at 10 cm height to form smooth gel beads. The gel beads were filtered, then put into a fresh $CaCl_2$ aqueous solution and kept at 4 °C for 2 h. The gel beads were filtered and washed with NaCl solution (0.9% w/v), then dried with absorbent paper and retained at 4 °C for O_2-tolerant test.

2.5. Anaerobic and aerobic hydrogen production from glucose

Method of anaerobic and aerobic hydrogen production from glucose was described in our previous study [32]. Main steps: (1) the strain cultured overnight was transferred into a new LB medium; (2) harvesting cells by centrifugation (6000×*g*, 5 min); (3) washing cells with pH 7.0 0.1 M PBS (containing 61 mM Na_2HPO_4 and 39 mM $NaH_2PO_4{\cdot}H_2O$); (4) adjusting cell concentration to OD_{600} = 1.0 by re-suspending the pellet in hydrogen production medium; (5) the suspension (20 mL) was transferred to a 140 mL serum bottle and sealed with a rubber stopper; (6) the air in the serum bottles was replaced with argon gas to create an anaerobic atmosphere (Note: 10% O_2 + 90% argon gas, air or 100% O_2 was injected into the serum bottle to replace argon gas in aerobic hydrogen production assay.); (7) serum bottles were incubated at 37 °C to allow cells to produce H_2; (8) the accumulated H_2 was detected by GC.

2.6. Analysis methods

The concentration of H_2 in collected gas was analyzed by gas chromatography (GC9790, Fuli Instrument Company, China) with a thermal conductivity detector. The method of H_2 quantification was described in our previous work [28,29]. Reducing sugars were estimated based on the Ghose method [35]. Protein concentration was quantified as described by Bradford [36].

2.7. Modeling

The three-dimensional structure model of KHyd3 large subunit was built via an automated protein homology-modeling service (SWISS-MODEL Workspace) [37]. The model was based on a template where the PDB ID was 3IAM-4 (Modeled residue range: 191–537 amino acid residues; sequence identity: 31.9%; *e*-value: 0.00e-1; QMEANscore: 0.41). The Ni–Fe center was manually inserted into the structural model based on template 1H2A-L (PDB ID) of *Desulfovibrio fructosovorans* [NiFe]-hydrogenase. Rendering of the Ni-Fe center was made with the PyMOL Version 1.3 (Schrödinger, LLC) (Fig. 2).

3. Results

3.1. Four key AARs (V125, V263, E340 and M362) of KHyd3 large subunit

Fifteen different AARs between KHyd3's large subunit and *E. coli* Hyd3's large subunit were explored according to homology comparison of their amino acid sequences. These different AARs between KHyd3 and *E. coli* Hyd3 were exchanged via site-directed mutagenesis technology. The O_2-tolerance of variants was analyzed using in vivo and in vitro methods described in Section 2.3.

Results of in vivo and in vitro assay were shown in Table 1. Four variants (V125I, V263Q, E340D and M362V) showed strikingly lower aerobic hydrogen evolving activity compared with their anaerobic hydrogen evolving activity. The RYY values were 5.7%, 8.0%, 8.8% and 5.5%, respectively, which were far lower than the corresponding value of the wild-type *K. oxytoca* HP1 (27.3%). After being exposed to air in solution for 24 h, RAA values of V125I (18.8%), V263Q (18.9%), E340D (17.3%) and M362V (16.4%) variants were significantly lower than the corresponding value of wild-type KHyd3 (24.8%). Additionally, corresponding *E. coli* variants (I125V, Q263V, D340E and V362M) were constructed to reversely verify these four AARs. Results also showed that all *E. coli* variants (I125V, Q263V, D340E and V362M) had less O_2-sensitivity comparing with wild-type *E. coli*, in particular the variant V362M (Table 1). These consistent results indicated that V125, V263, E340 and M362 were crucial for KHyd3's oxygen tolerance.

In contrast to wild-type *K. oxytoca* HP1, most variants showed lower anaerobic and aerobic hydrogen evolving activity except for variant T176D. Structure channels were not only for O_2, but also for H_2, H^+ and other molecules. Mutations of AARs would impact the diffusion rate of both O_2 and H_2, which means the rate of H_2 generation will also be affected to some extent. Therefore, most of variants presented lower activity than the wild-type one. The model of KHyd3 only covered the 191–537 amino acid residues out of the total 569 amino acid residues, while the amino acid residues of 1–190 and 538–569 were not included. Therefore, we could not confirm the respective position of T176D, H15N and Q82K at current stage. But there was visible difference between the side-chain of Thr (T) and Asp (D). The side-chain of Thr (T) was CH_3CHOH which was an uncharged polar residue, while the side-chain of Asp (D) was negatively charged polar residue. So if T176 located at the inner exit or outer entrance of gas channels, O_2 would be more likely to attach to Asp (D) than Thr (T). Likewise, higher RYY values of H15N and Q82K might caused by their side-chain's difference. For F447Y, its RYY value (28.14%) is only slight higher than that of the wild-type (27.27%), the difference is invisible. So F447 had not been considered as the key one.

3.2. The surface AARs affect the oxygen tolerance of KHyd3

According to the structure model of KHyd3 large subunit, V263, E340 and M362 were far from the Ni–Fe active center (Fig. 3A) but on the surface of the KHyd3 large subunit molecule (Fig. 3B). Therefore exchanges of V263Q, E340D and M362V were unlikely to affect the oxygen tolerance of the KHyd3 by altering the reductive potential of the Ni–Fe active center. Some studies deemed changing AARs of gas tunnel could alter [NiFe] hydrogenases' O_2-sensitivity by blocking O_2 access to the Ni–Fe active center [15–

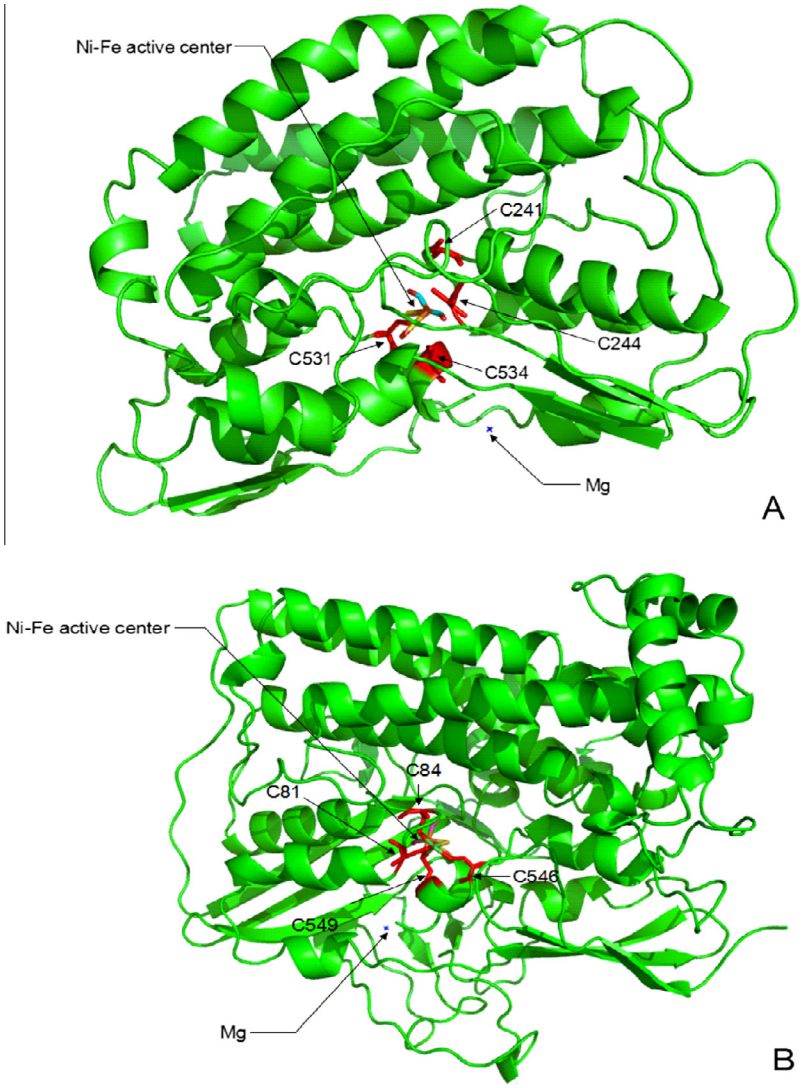

Fig. 2. Three-dimensional model of hydrogenase large subunit from *K. oxytoca* HP1 (A) and *D. fructosovorans* (B). The model template: 3IAM-4 (PDB ID); modeled residue range: 191–537; sequence identity [%]: 31.9%; *e* value: 0.00e-1; QMEANscore: 0.41. Red sticks: conserved Cys residues for coordinating [NiFe] active center; Rainbow sticks: [NiFe] active center. The Ni–Fe center was manually inserted into the structural model based on template 1H2A-L (PDB ID) of the *Desulfovibrio fructosovorans* [NiFe] hydrogenase. Rendering of the Ni–Fe center was made with the PyMOL Version 1.3 (Schrödinger, LLC). This model covered the 191–537 amino acid residues out of the total 569 amino acid residues, while the amino acid residues of 1–190 and 538–569 were not included. Similar to the *D. fructosovorans* [NiFe] hydrogenase large subunit (Fig. 2B), there were four strictly conserved Cys residues (C241, C244, C531 and C534) located at the center of the model to coordinate the Ni–Fe active center (Fig. 2A). Four long α-helices covered the top of the Ni-Fe active center, several short α-helices flanked the active sites and five β-sheets were at the bottom of the active center (Fig. 2A).

20]. However, all effective "gateway" AARs found were next to the Ni–Fe active center. No AARs were found at the surface of [NiFe]-hydrogenase molecules.

Further analysis revealed that M362 was located at the end of a long helix (Fig. 3A). Interestingly, M362 was just at the outer entrance of a gas tunnel (Fig. 3C). The corresponding location of this site in standard [NiFe]-hydrogenase (the O_2-insensitive one) from *D. fructosovorans* (PDB ID: 1FRF-L) was A417, which is also located at outer entrance of a gas tunnel (Fig. 3D) [38]. Although V263 and E340 are also located on the surface of KHyd3, they are not at the entrance of any hydrophobic tunnels (Fig. 3B). Thus the mechanism of how V263 and E340 affect the oxygen tolerance of KHyd3 was still unclear.

Dementin et al. [20] tested the effects on oxygen tolerance by replacing Val74 and Leu122 with methionines (Met) in the standard *D. fructosovorans* [NiFe]-hydrogenase. The results showed that the diffusion rate of O_2 decreased by more than two or even three orders of magnitude for single M mutant (V74M, L122M) and double MM mutant (V74M-L122M), respectively. There is visible difference between the side-chain of Met (M) and Val (V). The side-chain of Met (M) is $(CH_2)_2SCH_3$, while the side-chain of Val (V) is $CH(CH_3)_2$. On the one hand, the size of $(CH_2)_2SCH_3$ is larger than $CH(CH_3)_2$ (the molecular volume of Met was 30% larger than that of Val and about the same as Leu), which might make channel diameters smaller to restrict O_2 access to outer entrance of gas channels, working as the "gas sieve". On the other hand, "S" has high affinity with O_2, which may restrict O_2 access to outer entrance of gas channels by binding O_2. Whether polar AARs in this site, such as Glu (E), Asp (D), His (H), Arg (R), Lys (K), Asn (N), Gln (Q) or Tyr (Y), have a similar or stronger effect on the oxygen tolerance of KHyd3 compared with M362 was unclear and should be investigated in our future study.

From the structure model, we could see G300 and M362 shape an outer "gateway" of a gas tunnel (Fig. 3C). In order to further verify the key role of M362 for the O_2-tolerance of KHyd3 and determine how AARs' polarity or oxygen affinity acts on the oxygen

Table 1
Aerobic hydrogen evolving in vivo and oxygen-tolerance in vitro.

Variants[a]	Hydrogen yield in 24 h (mL)		RYY[g] (%)	Hydrogenase activity (U)		RAA[h] (%)
	100% Argon gas	10% O_2 + 90% Argon gas		0 h	24 h	
WT (K)[b]	14.34 ± 1.01	3.91 ± 0.28	27.27	267.76 ± 20.39	66.45 ± 4.61	24.82
I6L[c]	9.41 ± 0.70	2.60 ± 0.20	27.63*	259.35 ± 19.35	65.81 ± 5.16	25.37*
H15N[c]	8.02 ± 0.58	2.73 ± 0.22	34.30**	268.63 ± 16.34	63.40 ± 3.27	23.60*
Q16E[c]	13.74 ± 0.95	3.55 ± 0.25	25.84**	237.84 ± 18.91	60.14 ± 4.73	25.28**
E25H[c]	9.08 ± 0.63	1.68 ± 0.09	18.50**	242.11 ± 25.55	60.53 ± 3.05	25.00*
Q82K[c]	10.40 ± 1.12	4.04 ± 0.41	38.90**	213.35 ± 15.70	47.68 ± 3.63	22.36*
V125I[c]	7.77 ± 0.83	0.44 ± 0.06	5.66**	200.64 ± 10.90	37.82 ± 1.92	18.84**
T176D[c]	16.01 ± 0.94	5.07 ± 0.45	31.67**	225.00 ± 14.47	65.79 ± 3.29	29.24**
V263Q[c]	8.95 ± 1.02	0.72 ± 0.08	8.04**	156.60 ± 10.06	29.56 ± 2.52	18.88**
E340D[c]	11.42 ± 0.75	1.00 ± 0.09	8.76**	192.81 ± 11.11	33.33 ± 3.27	17.29**
D355E[c]	11.73 ± 0.83	1.93 ± 0.12	16.45**	247.33 ± 16.00	65.33 ± 4.67	26.42**
M362V[c]	8.55 ± 0.94	0.47 ± 0.05	5.50**	187.58 ± 11.76	30.72 ± 1.31	16.38**
Q382E[c]	9.79 ± 1.04	1.94 ± 0.13	19.82**	267.11 ± 21.05	56.76 ± 2.70	21.25*
T418E[c]	8.29 ± 0.58	1.99 ± 0.12	24.25*	245.70 ± 10.60	67.55 ± 2.65	27.49**
F447Y[c]	9.63 ± 0.46	2.71 ± 0.15	28.14*	224.14 ± 15.17	55.48 ± 4.52	24.75*
S474A[c]	11.74 ± 0.62	2.96 ± 0.18	25.21**	259.29 ± 22.14	57.86 ± 5.71	22.31*
WT (E)[d]	5.15 ± 1.11	0.82 ± 0.05	15.92	92.14 ± 8.27	ND[f]	/
I125V[e]	5.33 ± 0.65	1.37 ± 0.08	25.70****	100.00 ± 7.26	ND[f]	/
Q263V[e]	5.03 ± 0.73	1.13 ± 0.04	22.47****	97.14 ± 8.86	ND[f]	/
D340E[e]	5.24 ± 0.70	1.12 ± 0.02	21.37****	103.57 ± 9.29	ND[f]	/
V362M[e]	6.01 ± 0.75	1.51 ± 0.16	25.12***	107.14 ± 7.72	ND[f]	/

Each value is the mean of at least three replicates (±standard deviation). *P* values vs. WT (K) by *T*-test, $^{*}P < 0.05$, $^{**}P < 0.01$; *P* values vs. WT (E) by *T*-test, $^{***}P < 0.05$, $^{****}P < 0.01$. Hydrogenase reaction system volume (2 mL): 200 μl purified enzyme, 1.8 mL Tris–HCl buffer (pH 7.5, 50 mM) with MV (1.5 mM), sodium dithionite (25 mM). The hydrogen production conditions were same as above.
"Hydrogenase activity (U)" means the total enzyme activity of the purified hydrogenase. Specific activity of purified hydrogenase (U/mg protein): Specific activity of purified hydrogenase (U/mg protein): 223.14 ± 17.00 (WT (K)), 216.13 ± 16.13 (I6L), 223.86 ± 13.62 (H15N), 198.20 ± 15.77 (Q16E), 201.75 ± 19.00 (E25H), 177.70 ± 16.52 (Q82K), 167.20 ± 10.68 (V125I), 187.50 ± 12.06 (T176D), 130.50 ± 8.39 (V263Q), 160.68 ± 9.26 (E340D), 206.11 ± 13.33 (D355E), 156.32 ± 9.80 (M362V), 222.59 ± 17.54 (Q382E), 204.75 ± 8.83 (T418E), 186.78 ± 14.37 (F447Y), 216.07 ± 18.45(S474A), 76.79 ± 8.42 (WT (E)), 83.88 ± 9.30 (I125V), 80.95 ± 7.53 (Q263V), 86.31 ± 8.11 (D340E), 89.29 ± 6.55 (V362M).

[a] I: Ile; L: Leu; H: His; N: Asn; Q: Gln; E: Glu; K: Lys; V: Val; T: Thr; D: Asp; M: Met; F: Phe; Y: Tyr; S: Ser; A: Ala.
[b] WT (K): wild-type *K. oxytoca* HP1.
[c] Variants of *K. oxytoca* HP1.
[d] WT (E): wild-type *E. coil* K-12.
[e] Variants of *E. coil* K-12.
[f] ND: not detectable.
[g] RYY: ratio of aerobic hydrogen yield to anaerobic hydrogen yield, RYY (%) = (aerobic hydrogen yield in a given time/anaerobic hydrogen yield in a given time) × 100%.
[h] RAA: ratio of initial hydrogenase activity to residual hydrogenase activity, RAA (%) = (hydrogenase activity at a given time after exposure to air/the initial hydrogenase activity before exposure to air) × 100%.

tolerance of KHyd3, we constructed variants G300M (M300 and M362 shape an outer "gateway") and G300E (E300 and M362 shape an outer "gateway"). Results of O_2-tolerant assay in vivo and in vitro were listed in Table 2. Data of O_2-tolerant assay showed that both RYY and RAA were higher than that of wild-type KHyd3 (Table 2), in particular variant G300M. Another outer "gateway" L452 (Fig. 3E) was also changed to E452 and M452. Although L452E and L452M exhibited higher RYY and RAA compared with the wild-type strain (Table 2), lower anaerobic and aerobic hydrogen evolving yield of L452E and L452M made them poor candidates as O_2-tolerant hydrogenases.

3.3. The oxygen tolerance of KHyd3 varied with solution pH, immobilization and concentration of O_2 in the atmosphere

We examined the effects of different pH values on KHyd3's O_2-tolerance. This experiment was condition in this condition: Air (aerobic atmosphere), 4 °C. The results were shown in Fig. 4A. The enzyme activity of wild-type KHyd3 before O_2 exposure was 265.90 ± 17.30 U. We defined the enzyme activity of KHyd3 at the time 0 h was 100%. When the pH value of solution was as same as the pI value of KHyd3, the net charge on KHyd3 molecule surface was zero; when pH value was higher or lower than pI value, the net charge onKHyd3 molecule surface changed. We proposed that (1) the change of net charge on surface might facilitate or hinder O_2 access to KHyd3 molecule, which could lead to the change of KHyd3's O_2-telerance; (2) the change of net charge on surface might cause the enzyme molecule to loosen or tighten in structure to allow the O_2 easier or harder access to the active center through the hydrophobic gas channel. Thus, we conducted this pH experiment to test whether pH value could impact KHyd3's O_2-telerance. According to Fig. 4A, the line for pH 7.0 was much steeper than the other three from 0 h to 24 h, which meant that enzyme activity of KHyd3 in pH 7.0 decreased sharply than that of pH 5.0, pH 6.0 and pH 8.0. At the time 36 h, enzyme activities of KHyd3 in 4 different pH values were almost low as same, which showed that the protein structure of KHyd3 almost was destroyed after being exposed to air for 36 h. The pI value of KHyd3 was calculated as 6.72 using Compute pI/Mw tool (http://web.expasy.org/compute_pi/). The pH of 7.0 was considered to match the pI value of KHyd3; the net charge on the molecular surface at this pH value was the minimal compared with the other three. At this situation, the molecule structure of KHyd3 was much loosened than the other three, which might make the O_2 easier access to Ni–Fe center via the gas channel from the surface. Additionally, solvent pH values may affect hydrogenases' O_2-tolerance by modifying the surface charge of hydrogenase molecule, which would affect the O_2-affinity of AARs at the surface entrance of gas tunnels. These results indicate that the variation of solvent pH value can affect the O_2-tolerance of hydrogenases by modifying oxygen access to active center.

Immobilization could also modify the surface charge and the structure of the hydrogenase molecule. To investigate the effects of immobilization on O_2-tolerance of KHyd3, the hydrogenases were embedded with SA or absorbed by TiO_2 respectively. We

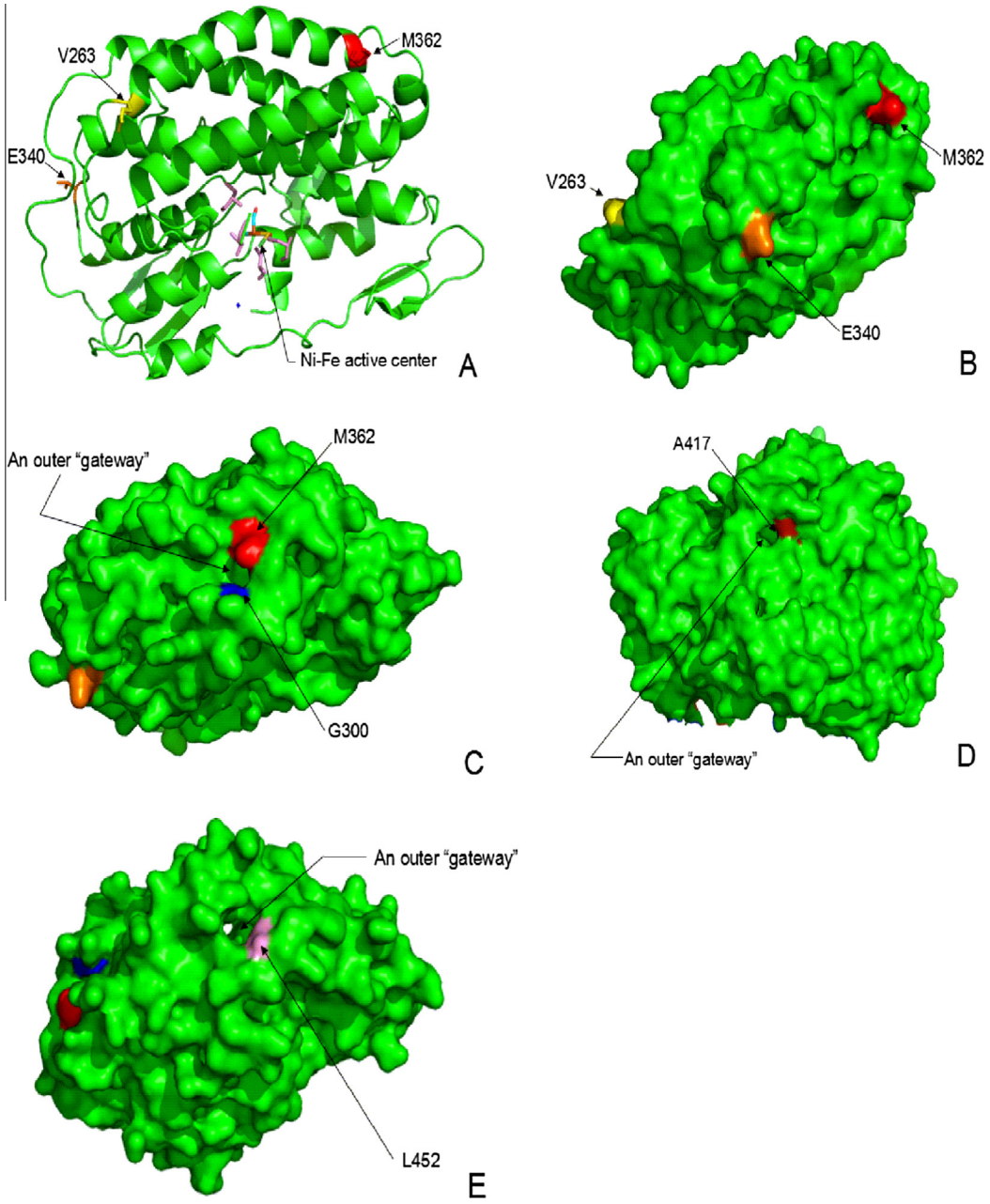

Fig. 3. The location of V263, G300, E340, M362 and L452 on KHyd3 large subunit model (A, B, C and E) and the location of A417 on *D. fructosovorans* [NiFe]-hydrogenase large subunit (D, PDB ID: 1FRF-L) [38]. Yellow: V263; Blue: G300; Orange: E340; Red: M362; Pink: L452; A417. The figures were prepared with the program PyMol.

Table 2
Surface amino acid residues at gas tunnel entrance affected aerobic hydrogen evolving in vivo and O_2-tolerance in vitro.

Variants	Hydrogen yield in 24 h (mL)		RYY (%)	Hydrogenase activity (U)		RAA (%)
	100% Argon gas	10% O_2 + 90% Argon gas		0 h	24 h	
KHyd3 (wild-type)	14.52 ± 1.07	3.87 ± 0.35	26.25	274.00 ± 26.00	66.23 ± 4.64	24.17
KHyd3 (G300E)	12.45 ± 0.50	4.64 ± 0.15	37.26**	262.50 ± 10.53	82.12 ± 1.99	31.28*
KHyd3 (G300M)	13.49 ± 0.41	5.15 ± 0.22	38.18**	269.80 ± 14.77	83.44 ± 3.31	30.93*
KHyd3 (L452E)	10.05 ± 0.66	3.12 ± 0.11	31.04*	216.99 ± 17.65	61.59 ± 6.62	28.38**
KHyd3 (L452M)	10.29 ± 0.50	3.11 ± 0.13	30.22**	206.67 ± 23.33	58.55 ± 8.55	28.33**

Each value is the mean of at least three replicates (±standard deviation). *P* values vs. KHyd3 (wild-type) by *T*-test, $^{*}P < 0.05$, $^{**}P < 0.01$.
The hydrogenase reaction system was as same as that of Table 1.
The meanings of "hydrogenase activity (U)", "RYY" and "RAA" were as same as that of Table 1.
Specific activity of purified hydrogenase (U/mg protein): 232.20 ± 22.03 (KHyd3 (wild-type)), 222.46 ± 8.92 (KHyd3 (G300E)), 228.64 ± 12.51 (KHyd3 (G300M)), 183.89 ± 14.96 (KHyd3 (L452E)), 175.14 ± 19.77 (KHyd3 (L452M)).

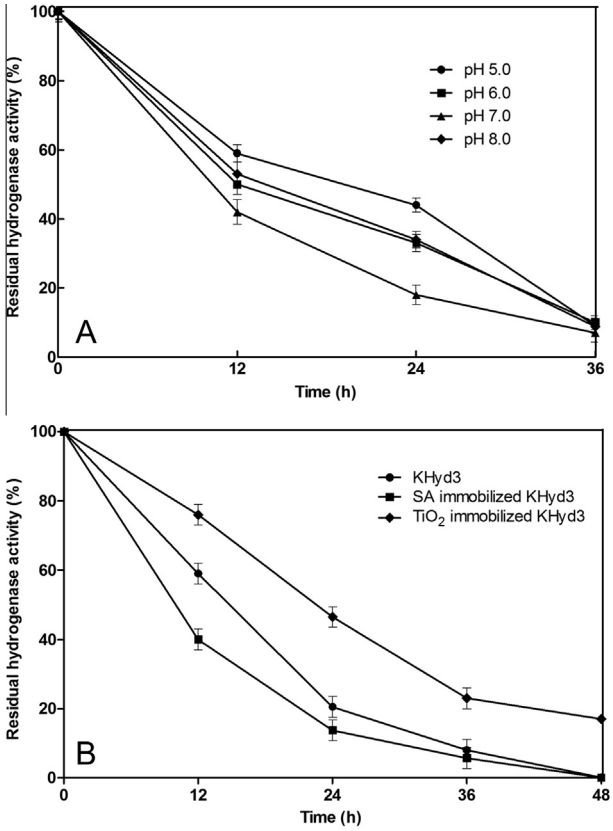

Fig. 4. Effects of pH (A) and immobilization (B) on O_2-tolerance of wild-type KHyd3. (A) This experiment was conducted in this condition: air (aerobic atmosphere), 4 °C. The enzyme activity of wild-type KHyd3 before O_2 exposure was 265.90 ± 17.30 U. We defined the enzyme activity of KHyd3 at the time 0 h was 100%. (B) This experiment was conducted under the condition of air (aerobic atmosphere) and 4 °C. At the time 0 h, the enzyme activity of KHyd3, SA immobilized KHyd3 and TiO_2 immobilized KHyd3 was 272.54 ± 19.00 U, 267.70 ± 16.80 U and 270.44 ± 14.59 U, respectively. The difference of enzyme activity at the time 0 h was invisible, we defined the enzyme activity of KHyd3, SA immobilized KHyd3 and TiO_2 immobilized KHyd3 at the time 0 h was 100%.

conducted this experiment in this condition: Air (aerobic atmosphere), 4 °C. The results were shown in Fig. 4B. At the time 0 h, the enzyme activity of KHyd3, SA immobilized KHyd3 and TiO_2 immobilized KHyd3 was 272.54 ± 19.00 U, 267.70 ± 16.80 U and 270.44 ± 14.59 U, respectively. The difference of enzyme activity at the time 0 h was invisible, we defined the enzyme activity of KHyd3, SA immobilized KHyd3 and TiO_2 immobilized KHyd3 at the time 0 h was 100%. At the time 24 h, compared with free KHyd3 (20.50%), residual activity of TiO_2 immobilized KHyd3 (46.50%) was significantly enhanced, whereas that of SA immobilized KHyd3 (13.70%) was slightly decreased (Fig. 4B). Even at the time 48 h, TiO_2 immobilized KHyd3 still showed 17.10% activity, while both free KHyd3 and SA immobilized KHyd3 lost the whole activity. Since the original enzyme activity of KHyd3, SA immobilized KHyd3 and TiO_2 immobilized KHyd3 before O_2 exposure (at the time 0 h) was at the similar level, the visible difference of activity at the time 48 h meant that immobilization may impact the O_2-tolerance of KHyd3 to some extent. The higher O_2-tolerance of the TiO_2-KHyd3 complex gave KHyd3 an advantage in hydrogen production by the photolysis of water. The O_2-tolerance of immobilized KHyd3 might have been affected by modifying the surface charge and surface structure of KHyd3.

Results in this paper regarding the effects of surface AARs, solvent pH values and the immobilization on O_2-tolerance of KHyd3 implied that the rate of O_2 access to the hydrogenase molecule was at least partly responsible for the O_2-tolerance of KHyd3.

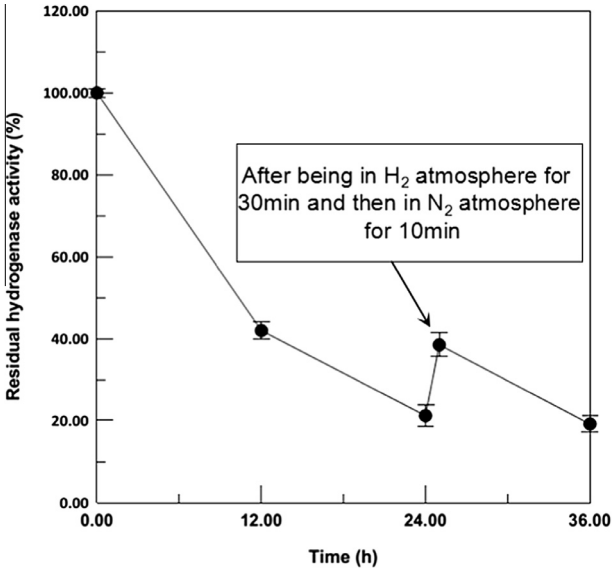

Fig. 5. Hydrogenase activity restored partly in an anaerobic atmosphere.

The relationship between oxygen partial pressure and the enzyme activity loss of KHyd3 was also displayed in Supplementary Fig. S3. After 48 h of exposure to oxygenic atmosphere, the enzyme activity loss of KHyd3 was relative to the oxygen partial pressure. The hydrogenase activity from in vivo tests was inversely related to the oxygen concentration of the atmosphere (Supplementary Table S2). Since the variation of oxygen partial pressure in atmosphere was unlikely to affect the structure of the hydrogenase molecules, the diffusion rate of O_2 access to the enzyme molecule was more likely to impact O_2-tolerance of KHyd3.

3.4. Hydrogenase activity restored partly in an anaerobic atmosphere

Early studies have shown that some O_2-inactivated [NiFe]-hydrogenases were able to restore their activity when being kept in an anaerobic atmosphere (H_2 or N_2) [23]. To determine if the O_2-inactivated KHyd3 could be reactivated after O_2 removal from the environment, the enzyme solution was exposed to air for 24 h, then the air atmosphere was replaced with pure H_2 for 30 min. The residual H_2 in the solution was removed by injecting N_2 for 10 min. Hydrogenase activity was monitored with time and the plot was displayed in Fig. 5. After exposure to oxygen for 24 h, the hydrogenase activity fell to 21.2% of its initial activity. The activity of KHyd3 rose to 38.5% after being kept in an anaerobic atmosphere for 40 min (H_2 for 30 min and N_2 for 10 min) (Fig. 5), but KHyd3 still could not restore the whole enzyme activity. In addition to O_2, there might be other factors that caused changes in the structure of KHyd3, so that the enzyme activity gradually lost. Although theoretically activity of O_2-inactivated [NiFe]-hydrogenase could be restored fully [23,39], actually it could only restore part activity. The results indicated that O_2-inactivated KHyd3 was able to partly restore its activity after O_2 was removed from the environment, which provided a basis for catalyzing aerobic hydrogen evolving in vivo.

4. Discussion

In past literatures, all key AARs for O_2-tolerance were at inner exit of gas channels next to active center, so we expected to find such AARs in KHyd3 because they might not only change channel diameters but also affect the oxidation–reduction potential of

active sites. However, key AARs (V263, E340 and M362) related to KHyd3's O_2-tolerance we found were all on the surface of its large subunit. Interestingly, it is the first time to find key AARs related to O_2-tolerance of hydrogenases on the surface. Particularly, M362 was at outer entrance of a gas tunnel. Results of experiments implied that rate of O_2 access to KHyd3 molecule was more likely to impact the O_2-tolerance of KHyd3 because surface AARs were unlikely to affect the oxidation–reduction potential of the Ni-Fe active center. Like O_2-tolerant H_2-sensing regulatory [NiFe]-hydrogenase (RH) from *Ralstonia eutropha* H16 [16] and O_2-tolerant H_2 sensor hydrogenases (SH) from *Desulfovibrio fructosovorans* [40,38,15], size of channel diameters also affected KHyd3's O_2-tolerance. Although key AARs of *R. eutropha* RH and *D. fructosovorans* SH located at the inner exit of gas channel, while crucial AARs of KHyd3's O_2-tolerance located at the outer entrance of gas channel, these AARs all affected the size of channel diameters to limit O_2 access to active center.

This study also showed that immobilization, O_2 partial pressure and the side-chain characteristics (polarity, hydrophobic, charge and bulk) of gas channel AARs might affect the O_2-tolerance of KHyd3 to some extent by altering the rate of O_2 diffusion. Combining our previous work [33] about the relationship between Fe-S clusters in small subunit of KHyd3 and KHyd3's O_2-tolerance and many reports about small subunit's Fe–S clusters [13,21–27], we concluded the final extent of KHyd3's final O_2-tolerance was determined by balancing the diffusion rate of O_2 access to the active sites and the deoxidation rate of the oxidized Ni–Fe active center.

Acknowledgements

This research was supported by the National Nature Science Foundation of China (Grant No. 31170760), the Natural Science Foundation of Fujian Province of China (Grant Nos. 2011J01219, 2013J01146) and by the National Science Foundation for Fostering Talents in Basic Research of the National Natural Science Foundation of China (Grant No. J1310027).

Appendix A. Supplementary data

Supplementary data associated with this article can be found, in the online version, at http://dx.doi.org/10.1016/j.febslet.2015.02.027.

References

[1] Lubitz, W., Ogata, H., Rudiger, O. and Reijerse, E. (2014) Hydrogenases. Chem. Rev. 114, 4081–4148.
[2] Weber, J. et al. (2014) Biotechnological hydrogen production by photosynthesis. Eng. Life Sci. 14, 592–606.
[3] Lojou, E., de Poulpiquet, A., Ranava, D., Mano, N., Giudici-Orticoni, M.T. and Gadiou, R. (2014). H_2 Production from Biomass for H_2/O_2 Biofuel Cells. in: Meeting Abstracts, The Electrochemical Society, pp. 982–982.
[4] Chenevier, P. et al. (2013) Hydrogenase enzymes: application in biofuel cells and inspiration for the design of noble-metal free catalysts for H_2 oxidation. C. R. Chim. 16, 491–505.
[5] Rousset, M. and Liebgott, P.-P. (2014) Engineering hydrogenases for H_2 production: bolts and goalsMicrobial BioEnergy: Hydrogen Production, pp. 43–77, Springer.
[6] Yagi, T. and Higuchi, Y. (2013) Studies on hydrogenase. Proc. Japan Acad. Ser. B 89, 16–33.
[7] So, K., Kitazumi, Y., Shirai, O., Kurita, K., Nishihara, H., Higuchi, Y. and Kano, K. (2014) Gas-diffusion and direct-electron-transfer-type bioanode for hydrogen oxidation with oxygen-tolerant [NiFe]-hydrogenase as an electrocatalyst. Chem. Lett. 43, 1575–1577.
[8] De Poulpiquet, A., Ciaccafava, A. and Lojou, E. (2014) New trends in enzyme immobilization at nanostructured interfaces for efficient electrocatalysis in biofuel cells. Electrochim. Acta 126, 104–114.
[9] Hamon, C., Ciaccafava, A., Infossi, P., Puppo, R., Even-Hernandez, P., Lojou, E. and Marchi, V. (2014) Synthesis and enzymatic photo-activity of an O_2 tolerant hydrogenase–CdSe@CdS quantum rod bioconjugate. Chem. Commun. 50, 4989.
[10] De Poulpiquet, A. et al. (2013) Exploring Properties of a Hyperthermophilic Membrane-Bound Hydrogenase at Carbon Nanotube Modified Electrodes for a Powerful H_2/O_2Biofuel Cell. Electroanalysis 25, 685–695.
[11] De Poulpiquet, A., Ciaccafava, A., Gadiou, R., Gounel, S., Giudici-Orticoni, M.T., Mano, N. and Lojou, E. (2014) Design of a H_2/O_2 biofuel cell based on thermostable enzymes. Electrochem. Commun. 42, 72–74.
[12] Xu, L. and Armstrong, F.A. (2015) Pushing the limits for enzyme-based membrane-less hydrogen fuel cells–achieving useful power and stability. Rsc Adv. 5, 3649–3656.
[13] Liebgott, P.-P., Dementin, S., Léger, C. and Rousset, M. (2011) Towards engineering O 2-tolerance in [Ni–Fe] hydrogenases. Energy Environ. Sci. 4, 33–41.
[14] Topin, J., Diharce, J., Fiorucci, S., Antonczak, S. and Golebiowski, J. (2014) O_2 migration rates in [NiFe] hydrogenases. A joint approach combining free-energy calculations and kinetic modeling. J. Phys. Chem. B 118, 676–681.
[15] Stiebritz, M.T. and Reiher, M. (2012) Hydrogenases and oxygen. Chem. Sci. 3, 1739–1751.
[16] Buhrke, T. (2005) Oxygen tolerance of the H_2-sensing [NiFe] hydrogenase from *Ralstonia eutropha* H16 is based on limited access of oxygen to the active site. J. Biol. Chem. 280, 23791–23796.
[17] Liebgott, P.-P., de Lacey, A.L., Burlat, B., Cournac, L., Richaud, P., Brugna, M., Fernandez, V.M., Guigliarelli, B., Rousset, M., Léger, C., et al. (2011) Original design of an oxygen-tolerant [NiFe] hydrogenase: major effect of a valine-to-cysteine mutation near the active site. J. Am. Chem. Soc. 133, 986–997.
[18] Oteri, F., Baaden, M., Lojou, E. and Sacquin-Mora, S. (2014) Multiscale simulations give insight into the hydrogen in and out pathways of [NiFe]-hydrogenases from *Aquifex aeolicus* and *Desulfovibrio fructosovorans*. J. Phys. Chem. B 118, 13800–13811.
[19] Cano, M., Volbeda, A., Guedeney, G., Aubert-Jousset, E., Richaud, P., Peltier, G. and Cournac, L. (2014) Improved oxygen tolerance of the *Synechocystis sp.* PCC 6803 bidirectional hydrogenase by site-directed mutagenesis of putative residues of the gas diffusion channel. Int. J. Hydrogen Energy 39, 16872–16884.
[20] Dementin, S., Leroux, F., Cournac, L., de Lacey, A.L., Volbeda, A., Leger, C., Burlat, B., Martinez, N., Champ, S., Martin, L., et al. (2009) Introduction of methionines in the gas channel makes [NiFe] hydrogenase aero-tolerant. J. Am. Chem. Soc. 131, 10156–10164.
[21] Fritsch, J., Scheerer, P., Frielingsdorf, S., Kroschinsky, S., Friedrich, B., Lenz, O. and Spahn, C.M.T. (2011) The crystal structure of an oxygen-tolerant hydrogenase uncovers a novel iron-sulphur centre. Nature 479, 249–252.
[22] Fritsch, J., Lenz, O. and Friedrich, B. (2013) Structure, function and biosynthesis of O_2-tolerant hydrogenases. Nat. Rev. Microbiol. 11, 106–114.
[23] Goris, T., Wait, A.F., Saggu, M., Fritsch, J., Heidary, N., Stein, M., Zebger, I., Lendzian, F., Armstrong, F.A. and Friedrich, B. (2011) A unique iron-sulfur cluster is crucial for oxygen tolerance of a [NiFe]-hydrogenase. Nat. Chem. Biol. 7, 310–318.
[24] Fritsch, J., Löscher, S., Sanganas, O., Siebert, E., Zebger, I., Stein, M., Ludwig, M., De Lacey, A.L., Dau, H. and Friedrich, Br. (2011) [NiFe] and [FeS] cofactors in the membrane-bound hydrogenase of *Ralstonia eutropha* investigated by X-ray absorption spectroscopy: insights into O_2-tolerant H_2 cleavage. Biochemistry 50, 5858–5869.
[25] Sigfridsson, K.G. (2015) Structural differences of oxidized iron-sulfur and nickel-iron cofactors in O_2-tolerant and O_2-sensitive hydrogenases studied by X-ray absorption spectroscopy. Biochim. Biophys. Acta (BBA)-Bioenerg. 1847, 162–170.
[26] Pandelia, M.-E., Bykov, D., Izsak, R., Infossi, P., Giudici-Orticoni, M.-T., Bill, E., Neese, F. and Lubitz, W. (2013) Electronic structure of the unique [4Fe-3S] cluster in O_2-tolerant hydrogenases characterized by 57Fe Mössbauer and EPR spectroscopy. Proc. Natl. Acad. Sci. 110, 483–488.
[27] Parkin, A. and Sargent, F. (2012) The hows and whys of aerobic H_2 metabolism. Curr. Opin. Chem. Biol. 16, 26–34.
[28] Minnan, L., Jinli, H., Xiaobin, W., Huijuan, X., Jinzao, C., Chuannan, L., Fengzhang, Z. and Liangshu, X. (2005) Isolation and characterization of a high H_2-producing strain *Klebsiella oxytoca* HP1 from a hot spring. Res. Microbiol. 156, 76–81.
[29] Wu, X.B., Liang, Y., Li, Q.Y., Zhou, J.A. and Long, M.N. (2011) Characterization and cloning of oxygen-tolerant hydrogenase from *Klebsiella oxytoca* HP1. Res. Microbiol. 162, 330–336.
[30] Sauter, M., Bohm, R. and Bock, A. (1992) Mutational analysis of the operon (Hyc) determining hydrogenase-3 formation in *Escherichia-Coli*. Mol. Microbiol. 6, 1523–1532.
[31] Andrews, S.C., Berks, B.C., McClay, J., Ambler, A., Quail, M.A., Golby, P. and Guest, J.R. (1997) A 12-cistron *Escherichia coli* operon (hyf) encoding a putative proton-translocating formate hydrogenlyase system. Microbiol-Uk 143, 3633–3647.
[32] Bai, L.P., Wu, X.B., Jiang, L.J., Liu, J. and Long, M.N. (2012) Hydrogen production by over-expression of hydrogenase subunit in oxygen-tolerant *Klebsiella oxytoca* HP1. Int. J. Hydrogen Energy 37, 13227–13233.
[33] Huang, G.-F., Wu, X.-B., Bai, L.-P., Long, M.-N. and Chen, Q.-X. (2014) Enhanced oxygen tolerance of hydrogenase from *Klebsiella oxytoca* HP1 by Gly-Cys exchanges nearby Fe–S clusters as biocatalysts in biofuel cells or hydrogen production. Int. J. Hydrogen Energy 39, 18604–18611.

[34] You, C. and Zhang, Y.H. (2014) Simple cloning and DNA assembly in *Escherichia coli* by prolonged overlap extension PCR. Methods Mol. Biol. 1116, 183–192.
[35] Ghose, T. (1987) Measurement of cellulase activities. Pure Appl. Chem. 59, 257–268.
[36] Bradford, M.M. (1976) A rapid and sensitive method for the quantitation of microgram quantities of protein utilizing the principle of protein-dye binding. Anal. Biochem. 72, 248–254.
[37] Arnold, K., Bordoli, L., Kopp, J. and Schwede, T. (2006) The SWISS-MODEL workspace: a web-based environment for protein structure homology modelling. Bioinformatics 22, 195–201.
[38] Volbeda, A., Montet, Y., Vernède, X., Hatchikian, E.C. and Fontecilla-Camps, J.C. (2002) High-resolution crystallographic analysis of *Desulfovibrio fructosovorans* [NiFe] hydrogenase. Int. J. Hydrogen Energy 27, 1449–1461.
[39] Lamle, S.E., Albracht, S.P. and Armstrong, F.A. (2004) Electrochemical potential-step investigations of the aerobic interconversions of [NiFe]-hydrogenase from *Allochromatium v inosum*: insights into the puzzling difference between unready and ready oxidized inactive states. J. Am. Chem. Soc. 126, 14899–14909.
[40] Montet, Y., Amara, P., Volbeda, A., Vernede, X., Hatchikian, E.C., Field, M.J., Frey, M. and Fontecilla-Camps, J.C. (1997) Gas access to the active site of Ni-Fe hydrogenases probed by X-ray crystallography and molecular dynamics. Nat. Struct. Biol. 4, 523–526.